Journal of Molecular Liquids 288 (2019) 110999

Contents lists available at ScienceDirect

Journal of Molecular Liquids

journal homepage: www.elsevier.com/locate/molliq

Electrochemical behavior of polyaniline nanoparticles suspension: Adsorption and diffusion

Hadiseh Nazari, Reza Arefinia *

Chemical Engineering Department, Faculty of Engineering, Ferdowsi University of Mashhad, Mashhad, Iran

ARTICLE INFO

Article history:
Received 3 February 2019
Accepted 18 May 2019
Available online 26 May 2019

Keywords:
Polyaniline nanoparticle
Suspension
Diffusion
Adsorption
Electrochemical methods
Monte Carlo simulation

ABSTRACT

A stable suspension of polyaniline nanoparticles (nPANI) in acidic solution can be used in various applications. For the first time, the electrochemical behavior of nPANI as a dispersed phase in phosphoric acid (H_3PO_4) solution on a gold electrode has been investigated using a series of electrochemical methods including cyclic voltammetry (CV), chronoamperometry and electrochemical impedance spectroscopy. The prepared suspensions were stable during a long time. The electrochemical results confirmed two redox transformations within the nPANI structure occurred at the potentials of about 0.20 and 0.50 V (vs. Ag|AgCl) which are controlled by the irreversible diffusion and the adsorption mechanism of nPANI particles at the gold surface, respectively. Two main electrochemical parameters including total numbers of redox active sites per nPANI particle (4.2×10^5) and electron-transfer rate constant (9.7×10^{-6} cm s^{-1}) have been determined using CV method. The adsorption process of nPANI particles obeys Langmuir isotherm; additionally, the quantum chemical calculations and Monte Carlo simulation demonstrated that polyaniline macro molecules can replace water and phosphoric acid molecules from the surface upon its adsorption to the gold substrate. The surface analyses of the electrode using Raman spectroscopy, scanning electron microscopy and energy dispersive X-ray spectroscopy confirm the adsorption phenomenon.

1. Introduction

Polyaniline (PANI) is one of the mostly investigated and promising conducting polymers due to its facile synthesis, low cost monomer, tunable properties, reversible redox behavior and better stability compared to other conducting polymers [1–3]. During the recent several decades, a wide range of potential applications such as sensors [4], rechargeable batteries [5], fuel cells [6] and anti-corrosion agents [7,8] have been explored by conventional PANI. However, along with the development of nano science and technology, the nano-structured PANI reveals many novels or improved properties due to high surface area, high conductivity, as well as controllable chemical/physical properties. So it has been considered to be a promising nanomaterial candidate for the application in various fields [9,10].

In recent years, utilization of PANI as an applied film on the electrode surface has been attracted a great deal of attentions especially in the field of ion exchange applications due to the well doping and dedoping character of polyaniline [11–13]. In this regard, many efforts have been carried out to understand the redox properties of PANI films in various environments using different electrochemical techniques [14–17]. In addition, the effect of different dopant anions such as Cl^-, $H_2PO_4^-$, SO_4^{2-} has been studied on the redox properties of PANI films [11,16,18]. In the case of PANI films, the manufacturing process based on either electrochemical or chemical methods may be associated with some problems such as incomplete coverage of the electrode surface especially in the large-scale and also low mechanical properties of the prepared films.

To overcome these problems, dispersion of PANI particles in a solution may be a benefit and versatile method in the practical applications. According to the best our knowledge, no research has been done on this system subject to understand the electrochemical behaviors of PANI nanoparticles. However, the stability of such a suspension over the time may be a new challenge which could be improved by using the polyaniline particles in nano size as a dispersed phase.

In the present work, for the first time, the electrochemical behavior of nanopolyaniline (nPANI) particles dispersed in phosphoric acid solution (pH 2) was investigated on a gold electrode. For this purpose, various electrochemical methods including cyclic voltammetry (CV), chronoamperometry, electrochemical impedance spectroscopy (EIS) along with surface analyses methods including Raman spectroscopy,

* Corresponding author.
E-mail address: arefinia@um.ac.ir (R. Arefinia).

https://doi.org/10.1016/j.molliq.2019.110999
0167-7322/

scanning electron microscopy (SEM) and energy dispersive X-ray spectroscopy (EDS) have been employed. In addition, quantum chemical calculations and Monte Carlo simulation were adopted to add theoretical support for experimental results and investigate the adsorption mechanism.

Moreover, the specific of nPANI particles were characterized using dynamic light scattering (DLS) and Fourier transform-infrared spectroscopy (FT-IR) and the stability of the prepared suspension over time was checked using zeta potential measurement and UV–vis spectrum techniques.

2. Experimental

2.1. Materials and instruments

All chemicals were reagent grade and used as received without further purification and all of the aqueous solutions were prepared with double distilled water.

Electrochemical measurements were carried out by means of an Autolab potentiostat/galvanostat model 302 N with a conventional three electrodes system. The working electrode was a gold electrode (1 cm^2 in area). A platinum wire and a silver/silver chloride (Ag|AgCl) served as counter and reference electrode, respectively.

The chemical structure and average particle size of synthesized nPANI particles were characterized using FT-IR (Perkinelmer model spectrum 400) of dry powders and dynamic light scattering (DLS, Malvern) measurement in solution. The stability of nPANI solution was evaluated with zeta potential (Zeta Compact model, CAD, France) measurement and UV–vis (Cary model 50 Conc. spectrophotometer) spectrum.

After chronoamperometric test at 0.70 V (vs. Ag|AgCl) in nPD100 system, ex-situ Raman spectroscopy was performed with an AvaRaman-785 TEC with a 785 nm laser wavelength, exposure time 15 s, and laser power 800 mW. The scanning electron microscopy (SEM, LEO 1450VP) coupled with EDS were used to observe the surface of the gold electrode after electrochemical tests.

2.2. Synthesis of nPANI particles and preparation of suspensions

The nPANI particle was synthesized through the inverse microemulsion polymerization method according to that reported in our previous work [7,19].

All the electrochemical experiments were carried out in solutions prepared via dispersion of 5, 50 and 100 ppm nPANI ultrasonically suspended in 0.5 M aqueous phosphoric acid (H_3PO_4) solution and the pH value of solution was adjusted to 2 by NaOH.

The nPANI particles-dispersed in H_3PO_4 solution (pH 2) was signed as nPD following with a number which denotes the nPANI particle concentration e.g. nPD50 corresponds to the dispersion of 50 ppm nPANI in H_3PO_4 solution at pH 2.

2.3. Electrochemical experiments

Before electrochemical test, a gold electrode was carefully polished with alumina powder, sonicated in water and spent 10 min in a solution of 50 mM KOH and 25% H_2O_2. In addition, to clean the electrode surface, it was treated with cyclic voltammetry in the potential range from −200 to −1200 mV (vs. Ag/AgCl) once, at 50 mV/s scan rate in 50 mM KOH, and rinsed in Milli-Q water as described by Fischer et al. [20].

Voltammetric studies were performed in the potential range from −100 to 800 mV (vs. Ag/AgCl) for 10 cycles, at different scan rates (10, 30, 50 and 100 mV/s). Chronoamperometric measurements were carried out at a suitable potential with respect to the results obtained using CV test and the impedance measurements were immediately recorded after the chronoamperometric tests in a frequency range from 100 kHz to 0.01 Hz with an amplitude of voltage perturbation of 10 mV.

All electrochemical tests were performed at room temperature (25 ± 2 °C) and the prepared suspensions were thoroughly deoxygenated by application of a bubbling highly purified nitrogen, additionally a nitrogen atmosphere was maintained over the system during electrochemical measurements.

2.4. Quantum chemical study and Monte Carlo simulation

In the present study, the computational calculations were performed using the Material Studio v 8.0 Accelrys Inc. software. The quantum chemical calculations were performed with DMol^3 modulus based on density function theory (DFT). Geometrical optimization was accomplished with the generalized gradient approximation (GGA) functional of Becke's 3 parameter combined with Lee–Yang–Parr correlation (B3LYP) in conjunction with double Numerical plus polarization (DNP) basis set. Fine convergence criteria and global orbital cutoff were used on the basis set definitions. The adsorption behavior of polyaniline on Au (110) plane surface was investigated using Monte Carlo simulation via the adsorption locator module, COMPASS force field and periodic boundary conditions.

3. Results and discussion

3.1. Characterization of nPANI particles

Fig. 1 shows FT-IR spectrum of nPANI particles which is similar to those were reported in the literature [21,22]. Briefly, the characteristic peaks at 1560 cm^{-1} and 1475 cm^{-1} correspond to the quinoid (N═Q═N) and benzenoid (N—Q—N) ring stretching, respectively. The peaks at 1290 cm^{-1} and 1230 cm^{-1} are due to the C—N stretching.

The size of nPANI particles were determined using DLS test and shown in Fig. 2. It is clear that these particles have a narrow size distribution in a range between 40 and 60 nm.

3.2. Evaluation the stability of nPD system

The prepared suspension based on the dispersion of 100 ppm nPANI particles in H_3PO_4 at pH 2 (nPD100) was leaved under stagnant condition without exposure to atmosphere for two weeks and then its stability was checked using Zeta potential measurement. The measured value

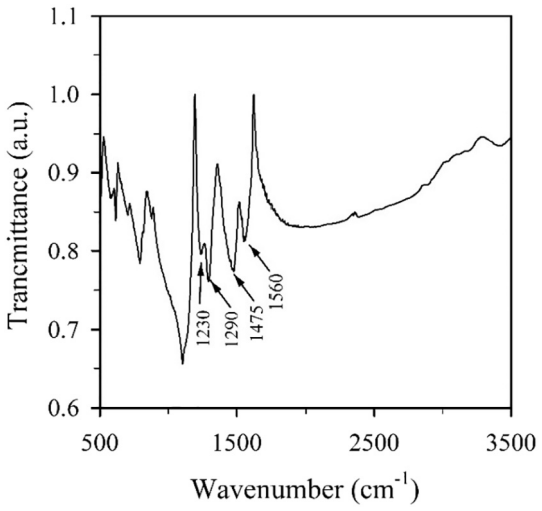

Fig. 1. FT-IR spectrum of nPANI particles synthesized via microemulsion polymerization method.

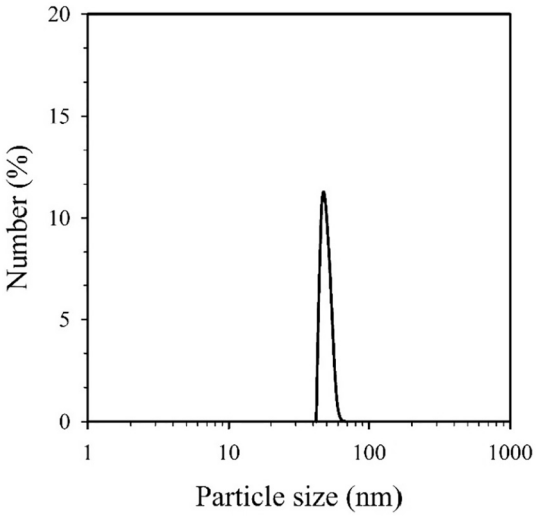

Fig. 2. DLS spectra of nPANI particles dispersed in H_3PO_4 solution.

of zeta potential was less than −30 mV which is a general indication of the fact that the system is an electrostatically stabilized suspension [23].

In the case of nPD systems, the suspension pH was adjusted at the value of 2 because of two main reasons: from one hand, at the lower pH values, the low dissociation constants of H_3PO_4 at room temperature [24], causes that the anion concentration probably will not be sufficient to made an efficient doping process of nPANI particles. On the other hand, at the higher pH values, the redox activity of polyaniline decreases and the redox peaks shift closer and overlap in the cyclic voltammetry measurements as described by Huang et al. [1]. Therefore, it seems that pH 2 is an adequate value to easily study the electrochemical behaviors of nPANI particles [24] at a sufficient content of ($H_2PO_4^-$) anions for participation in the doping/dedoping process.

The dispersion stability of nPD system with time was further evaluated by UV–vis spectroscopy. Fig. 3 shows a typical UV–visible absorption spectrum for the nPD100 system after 1 h and 2 weeks. It can be found that the spectra represent the characteristic absorption peaks of polyaniline where precisely discussed in our previous work [7]. Moreover, the negligible difference of spectra after 1 h and 2 weeks indicating that the concentration of nPANI particles within the suspension does not change during this time and thus the system is also physically a stabilized suspension.

3.3. Cyclic voltammetry technique

The electrochemical behavior of nPD system containing different concentrations of nPANI particles (blank, 5, 50 and 100 ppm) was studied using cyclic voltammetry technique and the tenth voltammetric cycle of nPD systems are shown in Fig. 4. It is apparent that in the absence of nPANI particles, there is no redox peak at the gold electrode surface within the potential window. However, in the presence of nPANI particles, the shape of CV curve recorded for all nPD systems is similar where involves an oxidation peak at about 0.20 V and a redox couple at higher potentials. These indicate that the electrolytic doping/dedoping process is associated with the electron transfer process as reported before in the case of polyaniline film [1,16,25–27].

The well-defined anodic wave with a half-wave potential at ca. 0.1 V (see Fig. 4) can be attributed to the conversion of leucoemeraldine (LE) to emeraldine salt (ES) whereas the cathodic wave for the reverse scan is very small and ill-defined [28]. This irreversibility may be due to insufficient reaction time during the nPANI/electrode collision [28].

The second voltammetric wave appears at about 0.50 V (see Fig. 4) corresponding to the oxidation of ES to the fully oxidized form of polyaniline (pernigraniline, PE) [25–27]. In this regard, Snauwaert et al. [29] have evidenced, by X-ray photoelectron spectroscopy, that the ratio between the amine and imine groups within the structure of PANI is a function of the electrochemical potential and the content of amine groups reduced by potential sweep in the positive direction. At the potential of 0.75 V (vs. Ag|AgCl), the polyaniline structure has the lowest amount of amine groups and hence ES is completely transformed to PE form.

Fig. 4 shows that the peak intensity increases gradually with increasing the nPANI particle concentration as a result of facilitating in the redox process near the electrode surface. Similar behavior was observed by Liu et al. [27] in the case of increase in the amounts of nPANI deposition on a glassy carbon electrode.

To study the redox reactions of nPANI particles-dispersed in H_3PO_4 solution, cyclic voltammetry for nPD100 system at different potential scan rates was performed and the tenth voltammetric cycles are shown in Fig. 5.

Fig. 5 shows that at all scan rates, the charge transfer for the 1st peak (LE → ES) occurs as an irreversible oxidation process. Moreover, the oxidation peak current was proportional to the square root of potential

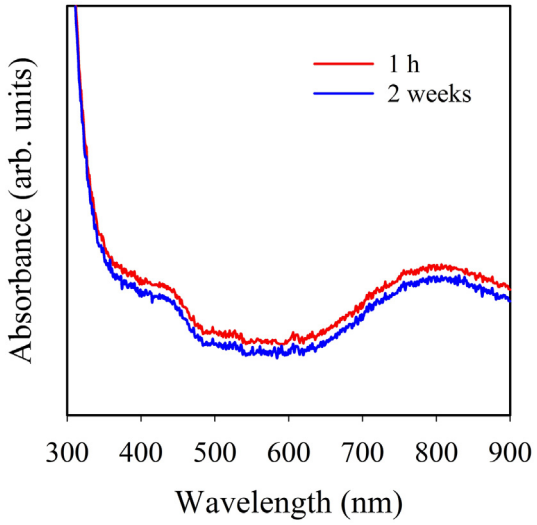

Fig. 3. UV–vis spectra of nPD100 system after 1 h and 2 weeks.

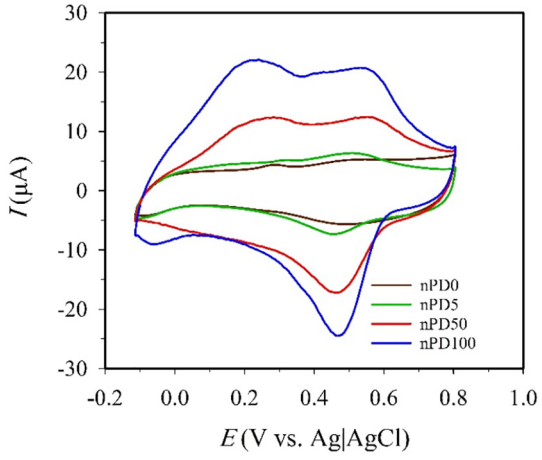

Fig. 4. Cyclic voltammograms of nPD system containing different concentrations (blank, 5, 50 and 100 ppm) of nPANI particles. Scan rate: 30 mV/s.

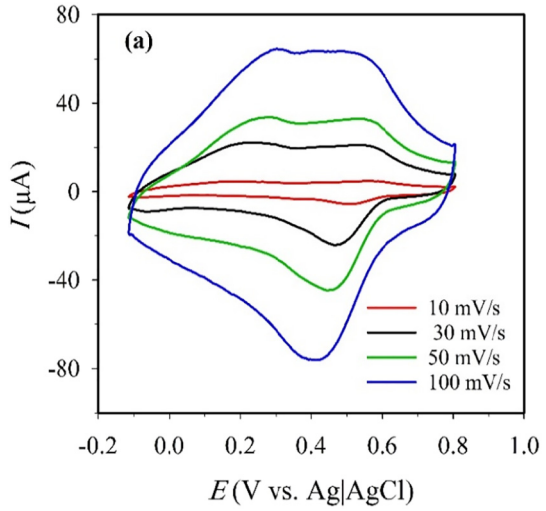

Fig. 5. Cyclic voltammograms of nPD100 system at different scan rates: 10, 30, 50 and 100 mVs^{-1} (from internal to external).

scan rate (figure has not been shown) with a correlation coefficient of about 0.99. Therefore, it can be found that the oxidation current is mainly controlled by the linear diffusion of nanoparticles [30], which can be quantified according to the following equation [31]:

$$I_p = \left(2.99 \times 10^5\right)(n'\alpha)^{1/2}\, n\, A\, c\, D^{1/2}\nu^{1/2} \quad (1)$$

where α is the charge transfer coefficient obtained from linear sweep voltammetry curve (not shown) according to Tafel equation [32], which is here estimated to be equal 0.69. The term n' is the number of the electron that simultaneously transferred during the redox reaction for a unit of reaction [28]. In the present work, it has been assumed that doping process i.e. incorporation of ($H_2PO_4^-$) anions occurs within a unit of reaction involving four neighboring aromatic rings and thus the value of n' equals 2. A is the electrode surface area (cm^2), c the concentration of nPANI particles (mol cm^{-3}), D the diffusion coefficient of nPANI particles estimated here to be 8.6×10^{-8} cm^2 s^{-1} from the Stokes-Einstein equation [28,33], ν the potential scan rate (V s^{-1}) and the parameter n corresponds to the total number of active redox sites per nPANI particle [28]. According to Eq. (1), the value of parameter n was estimated as 4.2×10^5 using the slope of I_p versus $\nu^{1/2}$ (not shown). The large value of n induces that nPANI particles could efficiently participate in the redox reaction (LE → ES) at the electrode surface.

The apparent electron-transfer rate constant (k^0) of nPANI particles-dispersed for the first oxidation step could be estimated using the slope of ln I_p vs. E_p according to the following equation [34]:

$$I_p = 0.227\, n\, FAc\, k^0\, \exp\left[-\frac{n'\alpha F}{RT}E_p - E^{0'}\right] \quad (2)$$

where I_p is the oxidation peak current, T the absolute temperature and $E^{0'}$ is the formal potential. F and R are the Faraday constant and the gas constant, respectively. Based on Eq. (2), the value of k^0 was calculated to be 9.7×10^{-6} cm s^{-1}. The low order of magnitude obtained for parameter k^0 approves that the conversion of LE to ES is associated with slow rate of electron transfer at the electrode surface and is a completely irreversible process which is in consistent with the absence of reduction peak for the first transformation of nPANI particles (Fig. 4).

At the second step of oxidation of nPANI particles shown in Fig. 5, when the scan rate increases, both anodic and cathodic peaks shift to more negative potentials additionally the anodic peaks become progressively broader. These observations support that the kinetic parameters have a great influence on the redox transformation of nPANI particles from ES to PE in H_3PO_4 solution [16].

The plot of log I_p vs. log ν for the second anodic peak is shown in Fig. 6, where the linear relationship with a good correlation (R^2 = 0.99) confirms the adsorption process of nPANI particles on the electrode surface as reported before by other researchers [35–37]. On the other hand, it can be found that the ratio of anodic to cathodic current at different scan rates (Fig. 5), deviates from unity and decreases with scan rate (figure has not been shown). These evidences indicate that the nPANI particles are mainly adsorbed as the ES form which was also reported by Wopschall et al. [38]. It can be suggested that the second redox peak is likely associated with three sequential steps: (a) adsorption of nPANI particles in the ES form, (b) oxidation reaction of ES to PE near the electrode surface and (c) diffusion of nPANI particles away from the electrode surface.

3.4. Chronoamperometry researches

To further study the electrochemical behavior of nPD system, the chronoamperometry method was employed in a different way from that commonly used for a polyaniline film-coated on the electrode surface [39–41]. In the other words, the chronoamperometric test for a polyaniline film is commonly performed in a two-step potentials involved early the complete reduction of film followed by an oxidation process at an appropriate potential. While, in the case of nPD systems, all of nPANI particles are initially in the ES form and they can be directly transformed using chronoamperometric test in a one-step potential.

Fig. 7a shows the chronoamperometric curves for nPD system at different concentrations of nPANI particles and at 0.70 V vs. Ag|AgCl, where the complete transformation of ES to PE occurs with respect to CV measurements shown in Fig. 4. As it is seen, for all nPD systems, the current density quickly decreases at the early times of oxidation process followed by a gradual reduction until reaches a stable value with no significant variations. Indeed, the decrease in the current density is attributed to the reduction in the concentration of ES form of nPANI particles near the electrode surface due to their consumption by the electrochemical reaction of redox transformation. Moreover, Fig. 7a shows that when the concentration of nPANI particles increases up to 100 ppm, the current density is finally stabled at the greater values as a result of higher adsorption rate of nPANI particles which favors the transformation of ES into PE.

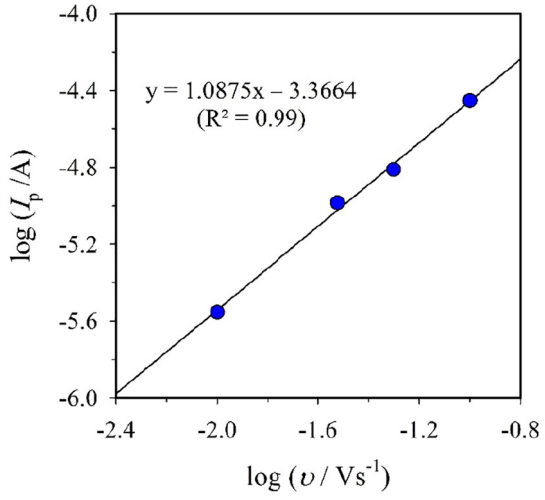

Fig. 6. The plot of log I_p vs. log ν for nPD100 system at the second anodic peak (ES → PE).

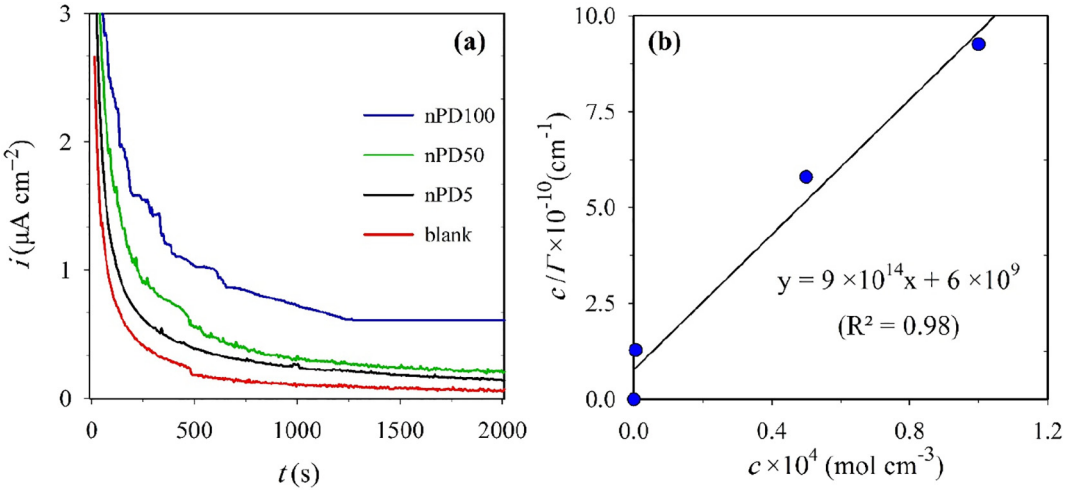

Fig. 7. Chronoamperograms of nPD system containing different nPANI particle concentrations, at the fixed potential of 0.70 V (vs. Ag|AgCl) (a). Langmuir adsorption isotherm for the nPD system at 0.70 V (vs Ag|AgCl) (b).

The adsorption phenomenon of nPANI particles in ES form on the gold surface can be thermodynamically analyzed by using the Langmuir isotherm as followed [42,43]:

$$\frac{c}{\Gamma} = \frac{1}{B\,\Gamma_{max}} + \frac{c}{\Gamma_{max}} \tag{3}$$

where Γ_{max} (mol cm^{-2}) is the maximum value of surface concentration and the parameter B (cm^3 mol^{-1}) represents the affinity of the nPANI particles towards the adsorption sites at a constant temperature. Γ (mol cm^{-2}) is the surface concentration of nPANI particles which can be calculated as following equation [43]:

$$\Gamma = \frac{Q}{n\,F} \tag{4}$$

where Q (C cm^{-2}) is the charge density produced by the transformation of nPANI particles from ES to PE during the adsorption process on the electrode. The value of this parameter can be calculated from the surface area beneath the chronoamperometric curves shown in Fig. 7a.

Fig. 7b shows the plot of c/Γ versus c where the linear behavior with a good coloration coefficient ($R^2 = 0.98$) confirms the validation of Langmuir isotherm for nPD system. With respect to the Eq. (4), the parameters Γ_{max} and B can be derived from the slope and intercept of plot of c/Γ versus c, respectively. Accordingly, the value of Γ_{max} and B are found to be 0.35 μg m^{-2} and 152 dm^3 mol^{-1}, respectively.

The Gibbs energy of adsorption (ΔG_{ads}, J mol^{-1}) for nPANI particles onto the electrode surface can be determined using the following equation [44]:

$$B = \frac{1}{0.055}\ \exp\left(-\frac{\Delta G_{ads}}{RT}\right) \tag{5}$$

where the value of 0.055 is the molar concentration of water (mol cm^{-3}). Using Eq. (5), ΔG_{ads} is −22 kJ mol^{-1} at 298 K. The negative value of Gibbs energy confirms the feasibility and the spontaneous nature of the adsorption of nPANI particles onto the gold electrode surface [45]. In addition, the value of ΔG_{ads} is around −20 kJ mol^{-1} suggesting the electrostatic interaction between nPANI particles and gold surface (physisorption) at 298 K, which is in agreement with that obtained by the cyclic voltammetry measurements.

Fig. 8 shows the chronoamperometric curves of gold electrode at different nPANI particle concentrations and at a potential (−0.10 V Ag|AgCl), that the complete transformation of ES to LE occurs with respect to Fig. 4. The negative sign of current density is originated from the reduction along with dedoping process. Moreover, the suddenly decrease of current density suggests the quickly transformation from ES to LE for the nPANI particles placed near the electrode surface. Fig. 8 shows that a steady-state value of current density is attained at different concentrations of nPANI particles under applied potential of −0.10 V for long times. This approves the fact that the process is likely controlled by the diffusion of nPANI particles from the bulk suspension towards the electrode surface.

Moreover, the inset of Fig. 8 shows that the current density response versus nPANI particle concentration is linear at various fixed times (100, 500, 1000 and 1500 s). In addition, the slope values of these plots are decreased by the increasing time elapsed. This approves that the transformation of ES to LE is mainly controlled by the diffusion of ES in the bulk solution which was previously reported for the ion diffusion in the case of PANI films [40], while it has not been addressed in the case of dispersed nPANI particles, additionally this observation is in good agreement with that obtained by the CV measurements (Fig. 5).

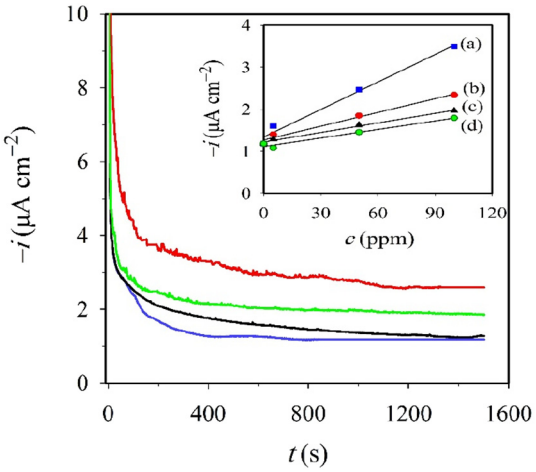

Fig. 8. Chronoamperograms of nPD system containing different nPANI particle concentrations (blank, 5, 50 and 100 ppm; from bottom to up), at the fixed potential of −0.10 V. Inset shows the dependence of the fixed-time current density (observed at 100 (a), 500 (b), 1000 (c) and 1500 s (d) after the potential step) versus nPANI particle concentration.

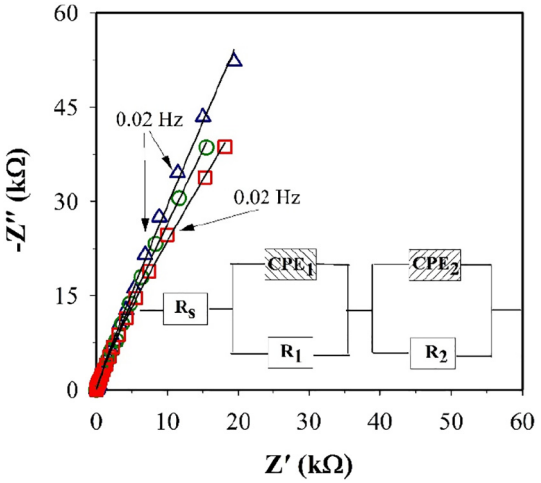

Fig. 9. Nyquist plots for a gold electrode recorded after chronoamperometric measurement at 0.70 V (vs. Ag|AgCl) in nPD system at (Δ) 5, (○) 50 and (□) 100 ppm nPANI, (—) fitting lines. Inset: Equivalent circuit used to fit the impedance data.

Table 1
Impedance parameters of nPD system at different nPANI particle concentrations.

Impedance parameter	nPD5	nPD50	nPD100
R_1 (Ω cm^2)	320	980	2208
C_1 (mF cm^{-2})	3.09	4.64	8.86
n_1	0.60	0.61	0.65
R_2 (kΩ cm^2)	991	331	252
C_2 (μF cm^{-2})	659	688	692
n_2	0.77	0.82	0.83

3.5. Impedance spectroscopy measurements

The electrochemical impedance spectroscopy (EIS) technique was employed to further study the interaction of nPANI particles with the gold surface.

Fig. 9 shows the Nyquist plots recorded at 0.70 V (vs. Ag|AgCl) for nPD system at different concentrations of nPANI particles.

The impedance data were well fitted with the equivalent circuit shown in the inset of.

Fig. 9 which was applied previously to explain the electrochemical behavior of conducting polymer film by Waller and Compton [46]. In this circuit, R_s is the solution resistance, the first sub-circuit (R_1//CPE$_1$) describes the interaction of the adsorbed nPANI particles-solution and the second sub-circuit (R_2//CPE$_2$) represents the interaction of the electrode- adsorbed nPANI particles. Therefore, R_1 is the ionic resistance associated to the redox process of the adsorbed nPANI particles. The CPE$_1$ (constant-phase element) is a pseudo capacitance element describes the contra-ion accumulation at the adsorbed nPANI particles-solution interface. Elements R_2 and CPE$_2$ correspond to the electronic charge transfer resistance and the double layer capacitance at the electrode-adsorbed nPANI particles interface, respectively.

Fig. 9 shows a good agreement between the experimental data (symbols) and fitting lines at all nPANI particle concentrations with respect to the equivalent circuit (shown in the inset of Fig. 9). The same was obtained when the spectra were presented in the form of a Bode and complex-admittance plot (not shown). The impedance parameters obtained by fitting procedure are presented in Table 1 where parameters C_1 and C_2 are the ideal capacitances calculated for CPE$_1$ and CPE$_2$ elements, respectively [47].

Table 1 shows that the increase of nPANI particle concentration results in an increase of both R_1 and C_1 values. These behaviors can be attributed to the accumulation of dopant anions ($H_2PO_4^-$) at the adsorbed nPANI particles-solution interface as a result of the dedoping process occurred during the transformation of ES to PE. Indeed, the increase of the dopant concentration causes two major effects: (a) make a repulsive force against further release of dopant anions where reasonably increases the ionic resistance (R_1) and (b) the increase of dielectric constant and thus the increase of C_1 [48].

Moreover, data presented in Table 1 shows a significant decrease of R_2 and a negligible increase of C_2 with the increasing the nPANI particles. Indeed, the increase in nPANI content provides higher adsorption of these particles on the electrode surface as obtained by the chronoamperometric test (Fig. 7). This evidence could be served as

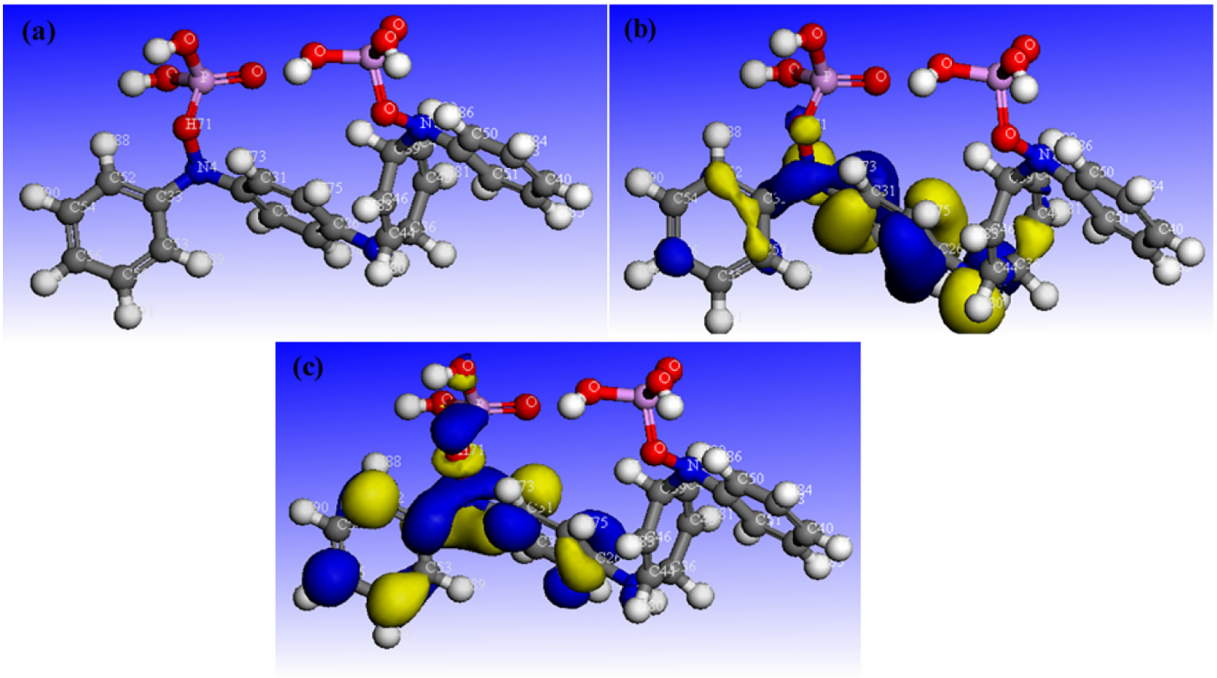

Fig. 10. The optimized structure (a), HOMO (b) and LUMO (c) distribution for polyaniline molecule.

the main reason for the reduction of electronic charge transfer and also increase of double layer capacitance (C_2).

More survey of data given in Table 1 shows that $R_1 < R_2$ and $C_2 < C_1$ indicating for the adsorbed nPANI particles the interaction with the electrode surface (charge transfer) is more important on the electroactive properties of nPANI particles compared to their interaction with solution (ionic transfer).

3.6. Quantum chemical study and Monte Carlo simulation

Quantum chemical calculations have been used to investigate the relationship between molecular and electronic structure of an organic molecule [49,50]. Fig. 10 shows the optimized structure, the highest occupied molecular orbital (HOMO) and the lowest unoccupied molecular orbital (LUMO) of polyaniline. The HOMO electron density is populated in the center of the molecule and in the benzenoid ring while the LUMO is observed in the vicinity of N atom and on the left side of the molecule according to optimized structure. It is predicted that for the electron donation driven adsorption, polyaniline may adsorb through the center of the molecule, whereas, if electron acceptation dominates the adsorption mechanism, polyaniline should adsorb through favorite LUMO sites [51].

To get a better understanding of the adsorption mechanism, Monte Carlo simulations were carried out in the presence of water/H_3PO_4 molecules on an Au (110) plane. The result of this simulation is shown in Fig. 11. As can be seen, polyaniline is able to overcome the water and phosphoric acid molecules and adsorb on the metal surface by replacing these molecules. This behavior is due to the affinity of polyaniline to adsorb at the gold surface, as was deduced from the free adsorption energy calculated in chronoamperometry research section. Moreover, the side view for the most stable adsorption configurations of polyaniline onto gold surface (in Fig. 11), predicts that polyaniline adsorb through favorite HOMO sites.

3.7. Surface study

The surface analyses were performed by Raman spectroscopy, SEM and EDS analysis after chronoamperometric test at 0.70 V (vs. Ag|AgCl) in nPD100 system followed by a thoroughly rinse of electrode surface with milli-Q water.

Fig. 12 shows the Raman spectra of electrode surface. The peaks at 1500 and 1589 cm^{-1} are ascribed to the C═C stretching deformations benzenoid and quinoid rings, respectively, and at 1176 cm^{-1} to a C—H bending vibration. The Raman bands at 1354, 805 and 517 cm^{-1} correspond to the quinoid ring [52–54]. These results clearly confirm the adsorption of nPANI particles on the gold electrode which is consistent with those obtained by both the CV and chronoamperometry experiments (Figs. 6 and 7).

Fig. 13 shows ex-situ characterization of the electrode surface by the SEM and EDS analysis. The existence of dark regions in SEM image is an indication of the adsorption of nPANI particles at the gold surface. Moreover, EDS analysis reveals the presence of carbon element in the dark regions while the bright regions are free of carbon (Fig. 13) which confirm the fact that nPANI particles have been adsorbed onto the surface of gold electrode. These observations satisfy the results obtained by both the CV and EIS methods.

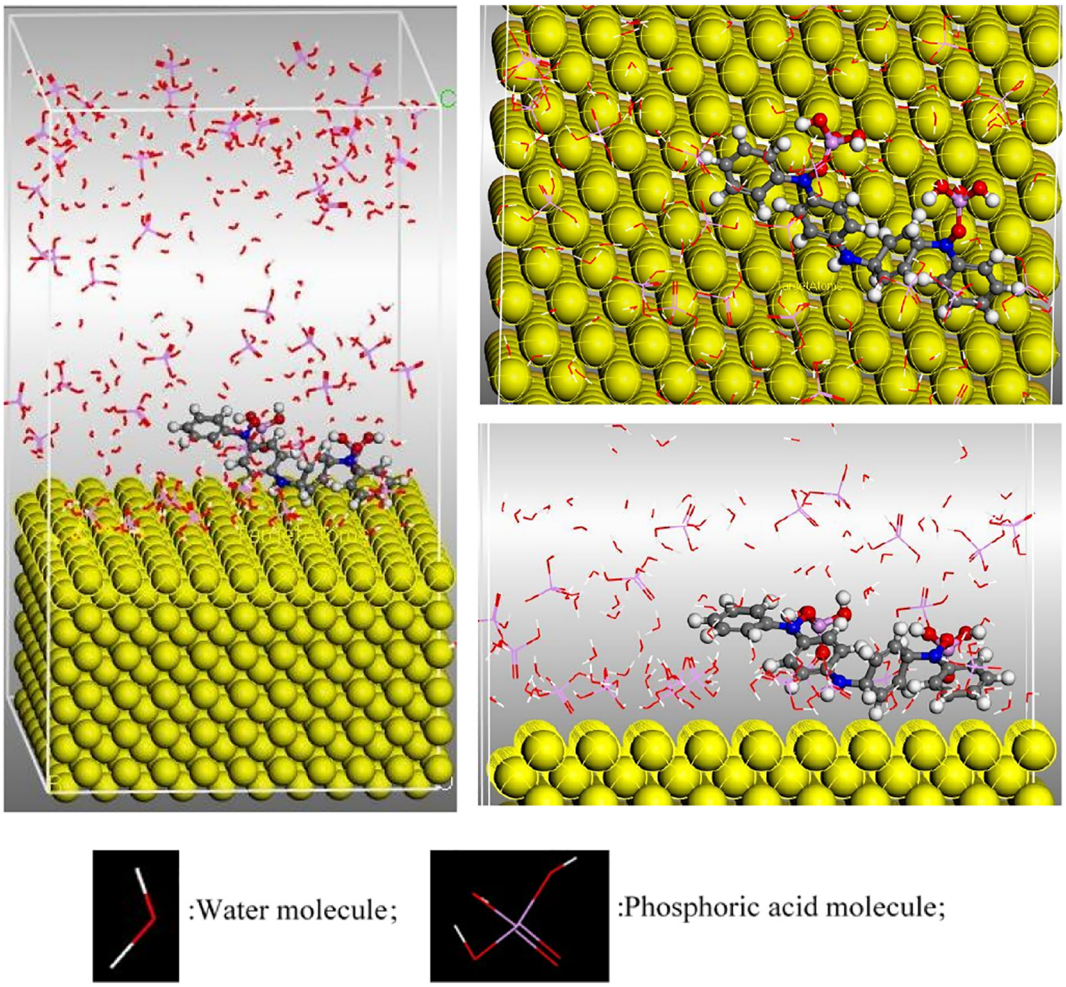

Fig. 11. Adsorption configuration of polyaniline in presence of water and phosphoric acid molecules on Au (110).

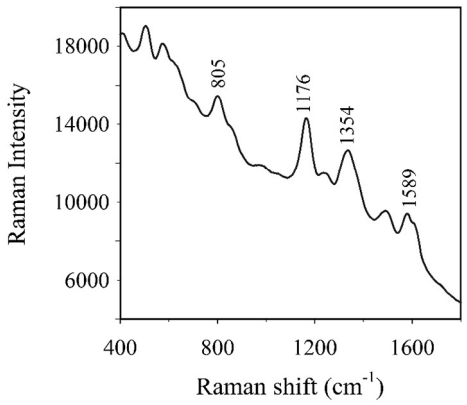

Fig. 12. Raman spectrum of nPANI adsorbed on the gold electrode surface at nPD100 system after chronoamperometric measurement at 0.70 V vs. Ag|AgCl.

4. Conclusions

The electrochemical behavior of nPANI particles-dispersed in H_3PO_4 solution (pH 2) was carefully investigated on a gold electrode. The nPANI particles display remarkable redox behavior and also doping/dedoping process in the suitable potential range and the main results are summarized as following:

- The nPANI suspensions had both the electrostatical and physical stability originated from the nano scale of particles along with the solubility feature induced by counter ions doping in H_3PO_4 solution.
- According to the voltammetric measurements, the LE form of nPANI particles converted to that ES around the peak potential of 0.20 V (vs. Ag|AgCl), where this transformation is controlled by an irreversible diffusion mechanism. At higher potentials around 0.50 V (vs. Ag|AgCl), there were a redox couple corresponding to the transformation of ES to PE under an adsorption-controlled mechanism. Furthermore, the chronoamperometry and EIS measurements indicate that the redox behavior of nPANI particles at the gold surface are controlled by the diffusion or adsorption phenomenon.
- The adsorption of nPANI particles obeys the Langmuir isotherm and the calculated thermodynamic parameters confirmed a physisorption of these particles. Moreover, the electrode surface was studied by Raman spectroscopy, SEM image and EDS analysis which verified the results obtained by electrochemical methods.
- Quantum and Monte Carlo simulations approved the hypothesis that polyaniline is able to adsorb on the gold surface by replacing

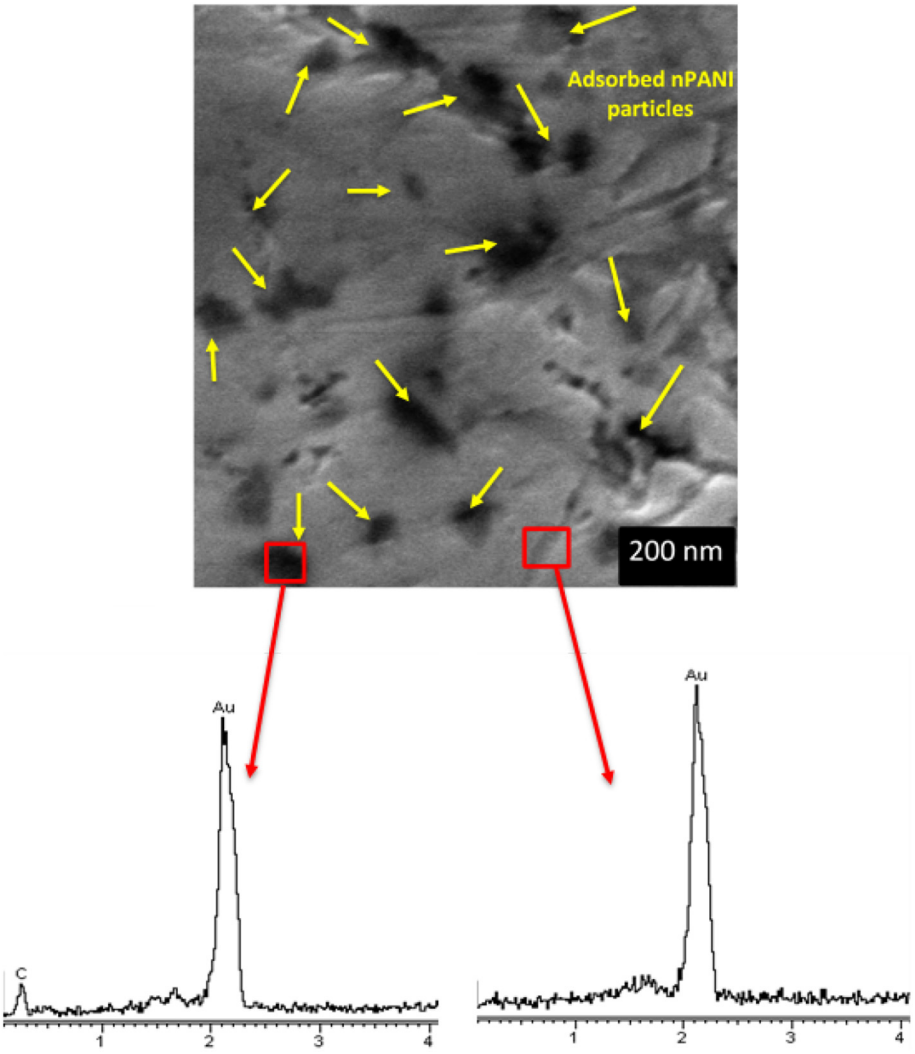

Fig. 13. SEM micrographs of the gold electrode surface at nPD100 system after chronoamperometric measurement at 0.70 V vs. Ag|AgCl. The arrows indicate adsorbed nPANI particles and bare gold surface, identified by EDS analysis.

the adsorbed water and phosphoric acid molecules.

- In summary, this work emphasizes the significant electrochemical performance of nPANI particles as a dispersed phase in acidic solution and suggests that this system could be a promising candidate serving as a substitute for the PANI films.

Acknowlegements

We highly appreciate Khorasan Razavi Gas Co. for their provision of laboratory facilities for conducting the experiments required in this research study. And we hereby acknowledge that part of this computation was performed on the HPC center of Ferdowsi University of Mashhad.

References

[1] W.S. Huang, B.D. Humphrey, A.G. MacDiarmid, Polyaniline, a novel conducting polymer. Morphology and chemistry of its oxidation and reduction in aqueous electrolytes, J. Chem. Soc. Faraday Trans. 82 (8) (1986) 2385–2400 1.
[2] Z.A. Boeva, V.G. Sergeyev, Polyaniline: synthesis, properties, and application, Polym. Sci. Ser. C. 56 (1) (2014) 144–153.
[3] G. Ćirić-Marjanović, Recent advances in polyaniline research: polymerization mechanisms, structural aspects, properties and applications, Synth. Met. 177 (2013) 1–47.
[4] M. Porcel-Valenzuela, J. Ballesta-Claver, I. de Orbe-Payá, F. Montilla, L.F. Capitán-Vallvey, Disposable electrochromic polyaniline sensor based on a redox response using a conventional camera: a first approach to handheld analysis, J. Electroanal. Chem. 738 (2015) 162–169.
[5] C.H. Tsao, C.H. Hsu, J.D. Zhou, C.W. Chin, P.L. Kuo, C.H. Chang, Vulcanized polymeric cathode material featuring a polyaniline skeleton for high-rate rechargeability and long-cycle stability lithium-sulfur batteries, Electrochim. Acta 276 (2018) 111–117.
[6] Y. Huang, C. Lin, C. Chang, M. Ho, Alternative platinum electrocatalyst supporter with micro/nanostructured polyaniline for direct methanol fuel cell applications, Electrochim. Acta 56 (16) (2011) 5679–5685.
[7] R. Arefinia, A. Shojaei, H. Shariatpanahi, J. Neshati, Anticorrosion properties of smart coating based on polyaniline nanoparticles/epoxy-ester system, Prog. Org. Coat. 75 (4) (2012) 502–508.
[8] M. Goyal, S. Kumar, I. Bahadur, C. Verma, E.E. Ebenso, Organic corrosion inhibitors for industrial cleaning of ferrous and non-ferrous metals in acidic solutions: a review, J. Mol. Liq. 256 (2018) 565–573.
[9] T. Lindfors, A. Ivaska, Application of Raman spectroscopy and sequential injection analysis for pH measurements with water dispersion of polyaniline nanoparticles, Anal. Chem. 79 (2) (2007) 608–611.
[10] D. Zhang, Y. Wang, Synthesis and applications of one-dimensional nano-structured polyaniline: an overview, Mater. Sci. Eng. B 134 (1) (2006) 9–19.
[11] Q. Hao, W. Lei, X. Xia, Z. Yan, X. Yang, L. Lu, X. Wang, Exchange of counter anions in electropolymerized polyaniline films, Electrochim. Acta 55 (3) (2010) 632–640.
[12] M. Lapkowski, E. Vieil, Control of polyaniline electroactivity by ion size exclusion, Synth. Met. 109 (1–3) (2000) 199–201.
[13] Y. Tang, K. Pan, X. Wang, C. Liu, S. Luo, Enhancing electrochemical and electrocatalytic activities of polyaniline via co-doping with poly (styrene sulfonate) and gold, J. Electroanal. Chem. 639 (1–2) (2010) 123–129.
[14] C. Barbero, R. Kötz, M. Kalaji, L. Nyholm, L. Peter, Ion exchange and memory effects in polyaniline, Synth. Met. 55 (2–3) (1993) 1545–1551.
[15] C. Barbero, M. Miras, R. Kötz, O. Haas, Comparative study of the ion exchange and electrochemical properties of sulfonated polyaniline (SPAN) and polyaniline (PANI), Synth. Met. 55 (2–3) (1993) 1539–1544.
[16] M. Gao, Y. Yang, M. Diao, S.g. Wang, X.h. Wang, G. Zhang, G. Zhang, Exceptional ion-exchange selectivity for perchlorate based on polyaniline films, Electrochim. Acta 56 (22) (2011) 7644–7650.
[17] Y.G. Han, T. Kusunose, T. Sekino, One-step reverse micelle polymerization of organic dispersible polyaniline nanoparticles, Synth. Met. 159 (1–2) (2009) 123–131.
[18] R.P. Kalakodimi, M. Nookala, Electrooxidation of ascorbic acid on a polyaniline-deposited nickel electrode: surface modification of a non-platinum metal for an electrooxidative analysis, Anal. Chem. 74 (21) (2002) 5531–5537.
[19] H. Nazari, R. Arefinia, An investigation into the relationship between the electrical conductivity and particle size of polyaniline in nano scale Inte, Int. J. Polym. Anal. Charact. 24 (2019) 1–13.
[20] L.M. Fischer, M. Tenje, A.R. Heiskanen, N. Masuda, J. Castillo, A. Bentien, J. Émneus, M.H. Jakobsen, A. Boisen, Gold cleaning methods for electrochemical detection applications, Microelectron. Eng. 86 (4–6) (2009) 1282–1285.
[21] B. Sreedhar, P. Radhika, B. Neelima, N. Hebalkar, M.B. Rao, Synthesis and characterization of polyaniline: nanospheres, nanorods, and nanotubes—catalytic application for sulfoxidation reactions, Polym. Adv. Technol. 20 (12) (2009) 950–958.
[22] G. Planes, J. Rodriguez, M. Miras, G. Garcia, E. Pastor, C. Barbero, Spectroscopic evidence for intermediate species formed during aniline polymerization and polyaniline degradation, PCCP 12 (35) (2010) 10584–10593.
[23] R. Hunter, Zeta Potential in Colloid Science, Academic Press, New York, 1981.
[24] D.A. Skoog, D.M. West, F.J. Holler, S. Crouch, Fundamentals of Analytical Chemistry, 9 ed. Nelson Education, 2013.
[25] H.-W. Park, T. Kim, J. Huh, M. Kang, J.E. Lee, H. Yoon, Anisotropic growth control of polyaniline nanostructures and their morphology-dependent electrochemical characteristics, ACS Nano 6 (9) (2012) 7624–7633.
[26] S. Pruneanu, E. Veress, I. Marian, L. Oniciu, Characterization of polyaniline by cyclic voltammetry and UV-vis absorption spectroscopy, J. Mater. Sci. 34 (11) (1999) 2733–2739.
[27] J. Liu, G. Zhu, X. Li, C. Batchelor-McAuley, S.V. Sokolov, R.G. Compton, Quantifying charge transfer to nanostructures: polyaniline nanotubes, Appl. Mater. Today 7 (2017) 239–245.
[28] K. Aoki, J. Chen, Q. Ke, S.P. Armes, D.P. Randall, Redox reactions of polyaniline-coated latex suspensions, Langmuir 19 (13) (2003) 5511–5516.
[29] P. Snauwaert, R. Lazzaroni, J. Riga, J. Verbist, D. Gonbeau, Electronic properties of conjugated polymers III, Springer Series in Solid State Sciences, 1989.
[30] E.-Y. Choi, J.W. Lee, J.J. Park, J.-M. Hur, J.-K. Kim, K.Y. Jung, S.M. Jeong, Electrochemical reduction behavior of a highly porous SIMFUEL particle in a LiCl molten salt, Chem. Eng. J. 207 (2012) 514–520.
[31] D.A. Brownson, C.E. Banks, The Handbook of Graphene Electrochemistry, Springer, 2014.
[32] D. Pletcher, R. Greff, R. Peat, L. Peter, J. Robinson, Instrumental Methods in Electrochemistry, Elsevier, 2001.
[33] C.A. Beasley, R.W. Murray, Voltammetry and redox charge storage capacity of ferrocene-functionalized silica nanoparticles, Langmuir 25 (17) (2009) 10370–10375.
[34] A.J. Bard, L.R. Faulkner, J. Leddy, C.G. Zoski, Electrochemical Methods: Fundamentals and Applications, wiley, New York, 1980.
[35] D. Santos, C. Sequeira, Cyclic voltammetry investigation of borohydride oxidation at a gold electrode, Electrochim. Acta 55 (22) (2010) 6775–6781.
[36] J.A. Ni, H.X. Ju, H.Y. Chen, D. Leech, Amperometric determination of epinephrine with an osmium complex and Nafion double-layer membrane modified electrode, Anal. Chim. Acta 378 (1–3) (1999) 151–157.
[37] L. Fotouhi, A.B. Hashkavayi, M.M. Heravi, Electrochemical behaviour and voltammetric determination of sulphadiazine using a multi-walled carbon nanotube composite film-glassy carbon electrode, J. Exp. Nanosci. 8 (7–8) (2013) 947–956.
[38] R.H. Wopschall, I. Shain, Effects of adsorption of electroactive species in stationary electrode polarography, Anal. Chem. 39 (13) (1967) 1514–1527.
[39] M.R. Nateghi, B. Savabieh, Study of polyaniline oxidation kinetics and conformational relaxation in aqueous acidic solutions, Electrochim. Acta 121 (2014) 128–135.
[40] G. Inzelt, Simultaneous chronoamperometric and quartz crystal microbalance studies of redox transformations of polyaniline films, Electrochim. Acta 45 (22–23) (2000) 3865–3876.
[41] L. Zhang, S. Dong, The electrocatalytic oxidation of ascorbic acid on polyaniline film synthesized in the presence of camphorsulfonic acid, J. Electroanal. Chem. 568 (2004) 189–194.
[42] H.N. Bhatti, A. Jabeen, M. Iqbal, S. Noreen, Z. Naseem, Adsorptive behavior of rice bran-based composites for malachite green dye: isotherm, kinetic and thermodynamic studies, J. Mol. Liq. 237 (2017) 322–333.
[43] M. Farcas, N.P. Cosman, D.K. Ting, S.G. Roscoe, S. Omanovic, A comparative study of electrochemical techniques in investigating the adsorption behaviour of fibrinogen on platinum, J. Electroanal. Chem. 649 (1–2) (2010) 206–218.
[44] D.R. Jackson, S. Omanovic, S.G. Roscoe, Electrochemical studies of the adsorption behavior of serum proteins on titanium, Langmuir 16 (12) (2000) 5449–5457.
[45] Y. Liu, Is the free energy change of adsorption correctly calculated? J. Chem. Eng. Data 54 (7) (2009) 1981–1985.
[46] A.M. Waller, R.G. Compton, Simultaneous alternating current impedance/electron spin resonance study of electrochemical doping in polypyrrole, J. Chem. Soc., Faraday Trans. 1 85 (4) (1989) 977–990.
[47] M. Piri, R. Arefinia, Investigation of the hydrogen evolution phenomenon on CaCO 3 precipitation in artificial seawater, Desalination 444 (2018) 142–150.
[48] H. Khani, R. Arefinia, Inhibition mechanism of nitrite on the corrosion of carbon steel in simulated cooling water systems, Mater. Corros. 69 (3) (2018) 337–347.
[49] R.E. Morsi, E. Khamis, A. Al-Sabagh, Polyaniline nanotubes: facile synthesis, electrochemical, quantum chemical characteristics and corrosion inhibition efficiency, J. Taiwan Inst. Chem. Eng. 60 (2016) 573–581.
[50] E. Naseri, M. Hajisafari, A. Kosari, M. Talari, S. Hosseinpour, A. Davoodi, Inhibitive effect of Clopidogrel as a green corrosion inhibitor for mild steel; statistical modeling and quantum Monte Carlo simulation studies, J. Mol. Liq. 269 (2018) 193–202.
[51] G. Gece, The use of quantum chemical methods in corrosion inhibitor studies, Corros. Sci. 50 (11) (2008) 2981–2992.
[52] S. Shreepathi, R. Holze, Spectroelectrochemistry and Preresonance Raman spectroscopy of polyaniline– dodecylbenzenesulfonic acid colloidal dispersions, Langmuir 22 (11) (2006) 5196–5204.
[53] A.H. Saheb, S.S. Seo, UV-vis and Raman spectral analysis of polyaniline/gold thin films as a function of applied potential, Anal. Lett. 44 (7) (2011) 1206–1216.
[54] Y. Furukawa, F. Ueda, Y. Hyodo, I. Harada, T. Nakajima, T. Kawagoe, Vibrational spectra and structure of polyaniline, Macromolecules 21 (5) (1988) 1297–1305.